Journal of Engineering Research and Reports

Volume 27, Issue 1, Page 123-139, 2025; Article no.JERR.127641
ISSN: 2582-2926

Analytic Determination of the Roller Length of a Hydraulic Jump in an Open Channel Flow Using a Bouncing Ball

Okechuku Ozueigbo [a*]

[a] *Department of Civil Engineering, Faculty of Engineering, University of Nigeria, Nsukka, Nigeria.*

Author's contribution

The sole author designed, analyzed, interpreted and prepared the manuscript.

Article Information

DOI: https://doi.org/10.9734/jerr/2025/v27i11373

Open Peer Review History:
This journal follows the Advanced Open Peer Review policy. Identity of the Reviewers, Editor(s) and additional Reviewers, peer review comments, different versions of the manuscript, comments of the editors, etc are available here: https://www.sdiarticle5.com/review-history/127641

Original Research Article

Received: 11/10/2024
Accepted: 15/12/2024
Published: 10/01/2025

ABSTRACT

A hydraulic jump is a natural occurrence that occurs in spillways, rivers, and other open channel flows when water or other liquid flowing with a high velocity discharges into a region of lower velocity with an attendant abrupt rise in the liquid surface. Such a phenomenon, known as hydraulic jump, is normally accompanied by substantial dissipation of energy. Many researchers, in the past, focus attention in the numerical study of the hydraulic jump, under varied working situations. Few attempts are made to study the occurrence analytically. In this paper, the author studied the incident analytically using a bouncing ball to develop a model to examine the lengths of hydraulic jumps in a horizontal open channel flow. The model development is based on the laws of motion, the principles of impulse and momentum, and the classical hydraulic jump formula. The model was later verified with the roller length obtained from the series of experiments conducted in a large-size facility. The roller length that the new model estimated compared well with the experimental results conducted within the Froude number ranges of 2.00 and 16.00. The model is ease to use and its accuracy as determined by the Pearson correlation coefficient is between 0.93 and 1.00.

**Corresponding author: Email: ozueigbo.okechukwu.pg78995@unn.edu.ng;*

Cite as: *Ozueigbo, Okechuku. 2025. "Analytic Determination of the Roller Length of a Hydraulic Jump in an Open Channel Flow Using a Bouncing Ball". Journal of Engineering Research and Reports 27 (1):123-39. https://doi.org/10.9734/jerr/2025/v27i11373.*

Keywords: Open channel flow; bouncing ball; hydraulic jump length; law of motion; froude number.

LISTS OF SYMBOLS

Fr - Froude Number;
Reynolds number defined as- Re = $\rho_w * U_w * D_H / \mu_w$
μ - dynamic viscosity (N.s/m^2);
ρ - density (kg/m^3);
v is the kinetic viscosity of water.
V_2 is the velocity of the ball at the positions 2 (m/s),
V_1 is the velocity of the ball at the positions 1 (m/s),
d_2 is the position of ball at location 2,
d_2 is the position of ball at location 2,
t, is the time of the ball's travel from positions 1 to 2 (s), g is the acceleration due to gravity (m2/s),
V_{avg} is the average velocity in a turbulent flow between two positions (m/s),
R is the hydraulic radius (m),
δ is the thickness of the boundary layer
v_* is the shear velocity and is given as
S is the water surface relative to the channel slope,
Lr is the roller length length of a hydraulic jump measured between positions 1 and 2 (m),
r is the Pearson Correlation Coefficient,
x and y are the values of the two variables.
n is the number of paired data points.
$\sum x$ is the sum of all x values.
$\sum y$ is the sum of all y values
$\sum x^2$ is the sum of the squares of x values.
$\sum y^2$ is the sum of the squares of y values.
$\sum xy$ is the sum of the product of corresponding x and y values.

1. INTRODUCTION

Hydraulic jump is an event that occurs when a high velocity fluid transitions from supercritical flow to subcritical flow (Peterka, 1978; Chanson, 2010; Carollo, 2012). It can also occur when steeper slopes lead to faster velocities, which can increase the likelihood and severity of a hydraulic jump or when channel geometry with steeper slopes leads to faster velocities, which can increase the likelihood and severity of a hydraulic jump or when channel geometry (narrow or constricted) channels may cause more dramatic jumps due to increased flow velocity (Boor, 1960; Busch, 1981; Chachereau & Chanson, 2010).

It is often observed in natural channels as well as in open channel manmade flow structures such as rivers and spillways (Chachereau & Chanson, 2011; Chanson, 2009; Chanson & Carvalho, 2015; Ciltrin, 1939; Einwechter, 1932). The flow is rapidly varied and is accompanied with substantial turbulence, splashes, kinetic energy dissipation, and intense air entrainment. The highly turbulent transition zone is usually referred to as the roller length and the start of the roller length, the jump toe or the impingement point; the jump toe is the point where the developing boundary layer intercepts the free surface and air in entrained there (Felder, & Chanson, 2018; Felder et al., 2021; Felder & Chanson, 2017; Hager & Bremen, 1989; Hager et al., 1990; Hager, 1992).

The Froude number is the primary factor in the determination of the nature of a hydraulic jump. It is given by the equation:

$$Fr_1 = \frac{V_1}{\sqrt{g d_1}} \quad (1)$$

Where:

V_1 is the approach flow velocity,
d_1 is the flow depth at position 1,
g is the gravitational acceleration.

In addition to the features of the channel bed such as roughness and slope, hydraulic jump properties can be influenced by scaling effects and by the inflow conditions (Montano & Felder, 2018; Montano & Felder, 2018; Ozueigbo, 2021).

A hydraulic jump is usually categorized by its inflow conditions based on the strength of the boundary layer development in the supercritical flows development upstream of the hydraulic

jump into undeveloped inflows (UD), partially developed inflows (PD), and fully developed inflow conditions (FD). The jump is classified based on the it's inflow Froude number into Undular when the inflow Froude number is between 1.0 and 1.7, Weak when the inflow Froude number is between 1.7 and 2.5, Oscillating when the inflow Froude number is between 2.5 and 4.5, Steady when the inflow Froude number is between 4.5 and 9.0, and Strong when the inflow Froude number is greater than 9.0 (Mossa, 1999; Mozer & Sevam, 2024).

The beneficial uses or applications of a hydraulic jump include:

i. Energy Dissipation: Hydraulic jumps are often used in spillways and energy dissipaters to reduce the energy of fast-moving water, preventing erosion and damage to downstream structures (Kucukali & Chanson, 2008; Leng & Chanson, 2015; Leutheusser & Alemu, 1979).
ii. Flow Regulation: Hydraulic jumps help in regulating flow characteristics, reducing the risk of damage caused by excessive flow speeds, particularly in river channels or artificial structures like sluice gates (Kramer et al., 2020, Kramer & Valero, 2020).
iii. Turbulence Induction: In some applications, hydraulic jumps are used deliberately to induce mixing or increase turbulence, such as in mixing chambers or aeration processes in water treatment facilities (Hoyt & Sellin, 1989, Kobus, 1980).

Fast sampling and fixed point instruments such as acoustic displacement meters (ADMs), Wire Gauges (WGs) are commonly used to measure the instantaneous free surface motions at a single fixed point per instrument (Montano & Felder, 2020), while LIDAR technology permits the concurrent and unbroken recording of the free surface motions with high spatial resolution, time-varying free-surface of hydraulic jumps including the average profiles, the minimum and maximum fee-surface elevations, the standard deviations and the characteristic frequencies along the hydraulic jump roller length (Li et al., 2020; Wang & Chanson, 2015b; Zhang et al., 2013; Ozueigbo & Agunwamba, 2023).

Li et al., (2021) showed that good agreement exists when these instruments were used to measure the free surfaces properties such as elevations, fluctuations, skewness, kurtosis, and frequencies, as well as advanced free surface properties such as integral time and length scales.

Researchers have used point instruments with the phase detection intrusive probe and video based detection to measure the free surface properties. Their studies concentrated either on the turbulent water flow properties with relatively low Froude number situations or on the air-water flow properties in the jump roller length (Ozueigbo & Agunwamba, 2023).

Analytic modeling of hydraulic jumps was the subject of a few researches, while the air-water flow parameters were examined under a few specific circumstances. The size and temporal scales of turbulent structures are essential details to explain turbulent processes, which is crucial for the advancement of analytic models and physical measurement methods (Murzyn & Chanson, 2009; Ohtsu & Yasuda, 1994; Rajaratnam, 1965; Rajaratnam, 1967).

Hence, this work aims to develop an analytic model of hydraulic jump for a wide range of flow with Froude numbers between 2.26 and 16.00.

2. EXPERIMENTAL CONFIGURATION

The experimental facilities, a vertical gate provided supercritical inflow. The height of the channel side walls was 2.5 m, such that the maximum inflow velocity was confined to 3.5 m/s. A constant head tank with a base 2 m x 2 m x 3 m high fed the channel. Discharges up to 250 l/s were run. The tank was divided by a vertical porous wall with Fig. 1. Inlet to (a) channel 3, (b) channels 1 and 4; longitudinal section. The transition from the tank to the channel was well rounded both along the sidewalls, along the tank bottom to the channel bottom (40 cm above it), and along the vertical, moveable gate. The inlet shape resembled a high-head intake. Further details on the experimental facility can be found in (Hager et al., 1990).

Table 1 summarizes the characteristics of selected experiments of hydraulic jump based on smooth bed condition The Reynolds number is defined as;

$$Re = 4V_1R/\nu \quad (2)$$

Where V_1 is the velocity, R as hydraulic radius at the toe of jump and ν is the kinetic viscosity of water. Characteristics of roller length observation for classical hydraulic jump (ν = 1.51 x 10^{-6} m^2s^{-1}).

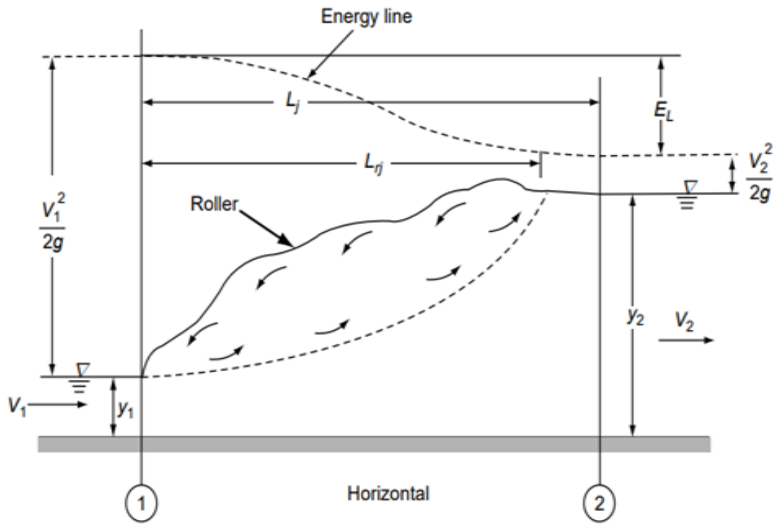

Fig. 1. Definition sketch of a hydraulic jump

Table 1. Characteristics of roller length observation for classical hydraulic jump (ν= 1.51 x 10^{-5} m^2s^{-1})

Author	b (cm)	d_1 (cm)	Fr_1	Re x10^{-5}	Formula
Safranez, (1929)	49.9	0.71 – 5.7	1.72 – 19.1	0.58 – 2.54	$\lambda_r = 6Fr_1$
Einwechter, (1932)	25.0	1.0 – 1.09	2.5 – 6.95	0.29 – 0.73	-
Pietrkowski, (1932)	10.0	0.5 – 1.46	5.5 – 19.8	0.83 – 1.72	$\lambda_r = 5.9F_{r1}$
Bakhmeteff & Matzke, (1936)	15.24	1.0 – 7.75	1.96 – 8.7	0.49 – 3.87	Diagram
Schroder, (1963)					
Rajaratnam, (1965)	59.8	3.4 – 10.2	1.83 – 9.93	4.44 – 10.6	$\lambda_r = 40\text{erf}$
	30.8	1.55 – 6.13	2.68 – 9.78	1.95 – 4.19	$\left[\frac{1}{16}(1+8Fr_1^2)^{0.5}-3\right]$
	16.7	1.36 – 3.18	3 – 6	0.86 – 9.88	
	33.3	1.98 – 0.70	3 – 6	1.71 – 7.31	-
Sarma & Newham, (1973)	50.0	0.66 – 8.04	3 – 6	0.35 – 17.3	-
Hager et al., (1990)	30.5	2.1 – 6.7	1.21 – 3.79	1.11 – 1.97	-
	50	5.4 – 54.7	2.88 –5.96	0.19 – 10.2	-
	50	5.4 – 54.7	2.88 – 5.96	0.19 – 10.2	$\lambda_r = 6.73(F_{r1}-1)$
					$\lambda_r = -12 + 160tanh(Fr_1/20)$
					$\lambda_r = -12 + 100tanh(Fr_1/12.5)$

These researchers used point-source measurements (Table 1).

3. METHODOLOGY

The author uses the existing rules of the Newton's Second Law of Motion, the continuity and momentum equations, and the classical hydraulic jump equation to build this model (Bélanger, (1841). He uses the equation of motion to calculate the trajectory of an elastic pinball as it bounces on a plain horizontal surface and compares it to the profile of a flow with a hydraulic jump (Fig. 2).

2a) The motion of a bouncing ball obeys projectile motion the following forces act on a ball during its flight: gravitational force, drag force due to air resistance, Magnus force due to the ball's spin, upwards buoyance force due to the ball's immersion in air. Usually, the Newton's second law of motion considering all forces is used to study the motion of a ball. Because the other forces are normally small, the motion of a ball is frequently idealized as being influenced only by the gravitational force (Cross, 2019; Cross & Crawford, 2019).

If it is only the gravitational force that acts on the ball, the mechanical energy will be conserved

during its flight. In this case, the equations of the motion of a ball are given by:

$$V_2 = V_1 + gt \quad (3)$$

$$d_2 = d_1 + V_1 t + \frac{1}{2} g t^2 \quad (4)$$

Simplifying (4), gives t as

$$t = \sqrt{2d_1\,(d_2/d_1 - 1)/g} \quad (5)$$

$$or\ t = \sqrt{2d_1\,A/g} \quad (6)$$

Where

$$A = (d_2/d_1 - 1) \quad (7)$$

Where V_2 and V_1(the velocity) and $d_2$and d_1 (the position) represent the velocities and locations of the ball at the positions 2 and 1 respectively, while t, is the time of the ball's travel from positions 1 to 2, and g is the acceleration due to gravity.

2b) According to Giles et al., (1994), the average velocity of flow in a turbulent flow for a wide channel with smooth surfaces, is given as;

$$V_{avg} = 2.5 v_* \, ln(41.2\, R/\delta) \quad (8)$$

Where V_{avg} is the average velocity in a turbulent flow between two positions,

R is the hydraulic radius, which for a wide channel is d_1,

$$R = d_1 \quad (9)$$

δ is the thickness of the boundary layer and is given as;

$$\delta = 11.6\, \nu / v_* \quad (10)$$

Where,

v_* is the shear velocity and is given as,

$$v_* = \sqrt{gSR} \quad (11)$$

S is the water surface relative to the channel slope and is given as;

$$S = (d_2 - d_1)/L_r \quad (12)$$

Where Lr is the length of the hydraulic jump measured between positions 1 and 2.

Substituting (9) and (10) in (12) and simplifying gives v_*, the shear velocity as;

$$v_* = \sqrt{g d_1^2\, A/L_r} \quad (13)$$

Substituting (13) in (10) and simplifying gives

Substituting (9) and (11) in (6) and simplifying gives δ as;

$$\delta = 11.6\, \nu / \left(\sqrt{g d_1^2\, A/L_r}\right) \quad (14)$$

Substituting (9), (13), and (14) in (8), and simplifying gives V_{avg} as;

$$V_{avg} = 2.5 d_1 \sqrt{\frac{gA}{L_r}}\, ln\left(41.2 d_1^2 \frac{\sqrt{g\,A/L_r}}{11.6\upsilon}\right) \quad (15)$$

2c) Pearson Correlation Coefficient, a popular statistical analysis, is used to evaluate the accuracy of the developed model. The Coefficient is a linear correlation coefficient that returns a value of between -1 and +1. -1 means a strong negative correlation, 0 is there is no correlation and +1 there is a strong positive correlation (Stephanie G. 2020).

The formula for the manual computation of Pearson's correlation coefficient is:

$$r = \frac{n\sum xy - \sum x \sum y}{\sqrt{(n\sum x^2 - (\sum x)^2)(n\sum y^2 - (\sum y)^2)}} \quad (16)$$

Where:

- x and y are the values of the two variables.
- n is the number of paired data points.
- ∑x is the sum of all x values.
- ∑y is the sum of all y values
- $\sum x^2$ is the sum of the squares of x values.
- $\sum y^2$ is the sum of the squares of y values.
- ∑xy is the sum of the product of corresponding x and y values

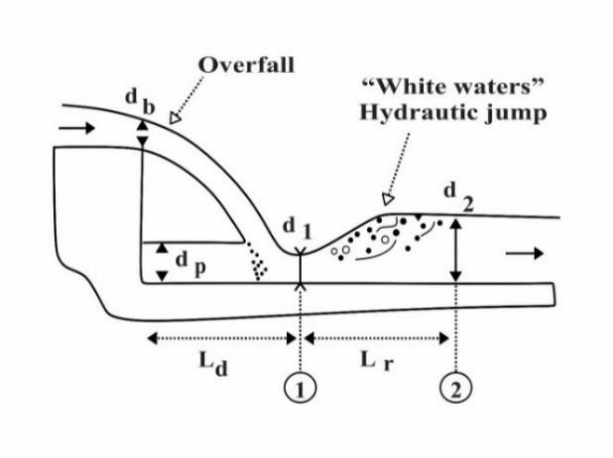

Fig. 2. Flow at a drop structure

4. FORMULATION OF THE MODEL

$$\frac{d_2}{d_1} = \frac{1}{2}\left[\sqrt{1+8Fr_1^2} - 1\right] \quad (17)$$

Equation (17) is a well-known classical hydraulic formula.

where the Fr_1 is the Froude number at position 1,

d is the water depth, g is the gravity constant, and the subscripts 1 and 2 are the upstream and downstream flow parameters, respectively.

Rearranging (17), yields

$$A = \frac{d_2}{d_1} - 1 = \frac{1}{2}\left[\sqrt{1+8Fr_1^2} - 1.5\right] \quad (18)$$

$$L_r = V_{avg}t \quad (19)$$

Substituting (6) and (15) in (19) and simplifying, yields

$$L_r = 2.5d_1\sqrt{\frac{gA}{L_r}}\sqrt{2d_1\,A/g}\;ln\left(41.2d_1^2\frac{\sqrt{gA/L_r}}{11.6\upsilon}\right) \quad (20)$$

Simplifying (20) further, yields

$$(L_r)^{1.5} = 3.536Ad_1^{1.5}ln\left(1.134d_1^2\sqrt{\frac{1}{L_r}}\frac{\sqrt{A}}{\upsilon}\right) \quad (21)$$

Where, $A = \frac{1}{2}\left[\sqrt{1+8Fr_1^2} - 1.5\right]$

Verification of the Developed Model: The author verifies the developed model (21) with the experimental roller length and the results are presented.

5. RESULTS AND DISCUSSION

5.1 Relationship between the Measured Roller Length and the Computed Roller Length of Fully Developed Hydraulic Jump Using the Developed Model (Eq 21)

Fig. 3a through Fig. 3h show the comparison of the measured roller length and the estimated roller length of a fully developed hydraulic jump with the Froude numbers between 2.26 and 15.96.

The figures show that the measured roller length compare well with the roller length computed with Eq (21) - the developed model with the Pearson correlation coefficients between 0.98 and 1.00.

The figures show that the measured and the developed model's roller length lengths increase rapidly with increasing Froude Numbers, which is in line with reports recorded in the literature.

5.2 Relationship between the Measured Roller Length and the Roller Length of Fully Developed Hydraulic Jumps Computed with the Developed Model (Eq 21)

Fig. 4a through Fig. 4h show the comparison of the measured roller length and the estimated roller length of fully developed hydraulic jumps predicted by the developed model (Eq 21) with the Froude numbers between 2.26 and 15.96.

The figures show that all the measured roller length compare well with the roller length computed with the developed model with the Pearson correlation coefficients between 0.93 and 1.00.

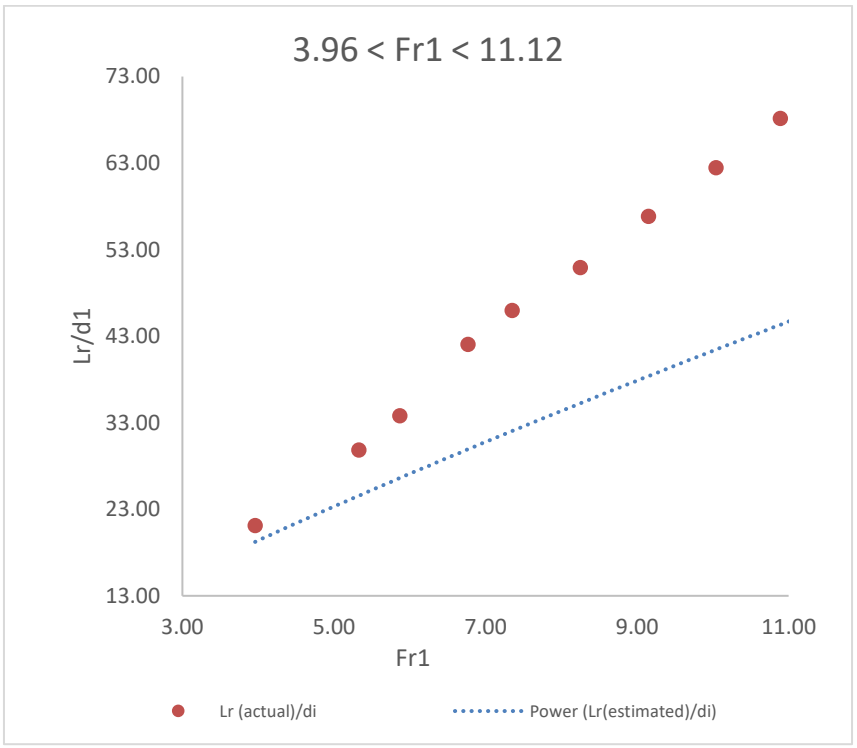

Fig. 3a. Froude number, Fr_1, of between 2.26 and 8.56 plotted as a function of the dimensionless hydraulic roller length length, Lr(estimated)/d_1 and Lr(measured)/d_1, of between 67 and 43. The Pearson Correlation Coefficient is 0.97

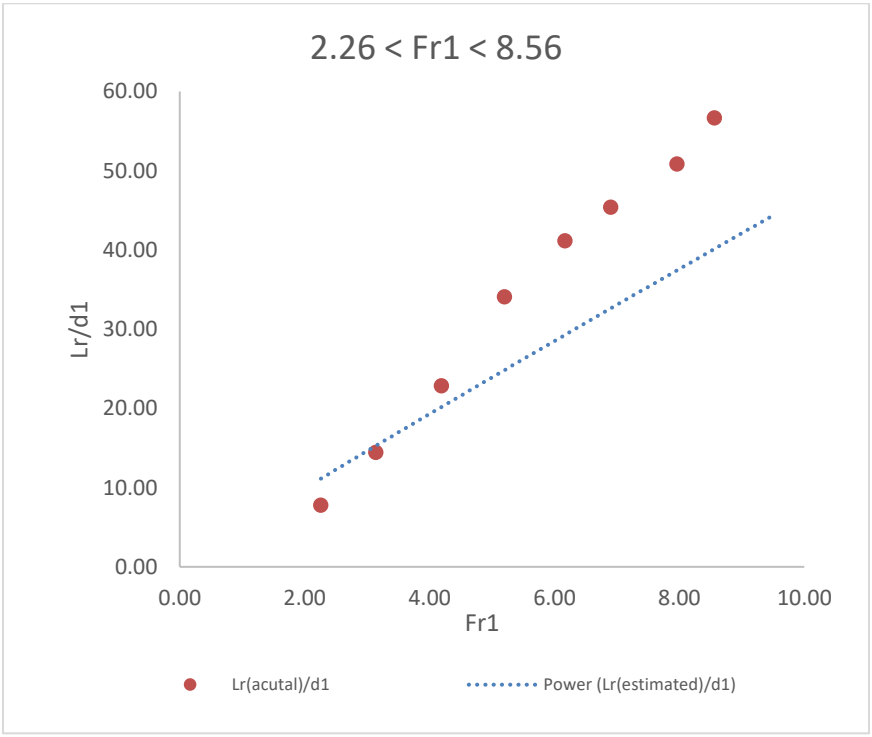

Fig. 3b. Froude number, Fr_1, of between 2.26 and 8.56 plotted as a function of the dimensionless hydraulic roller length, Lr(estimated)/d_1 and Lr(measured)/d_1, of between 57 and 38. The Pearson Correlation Coefficient is 0.97

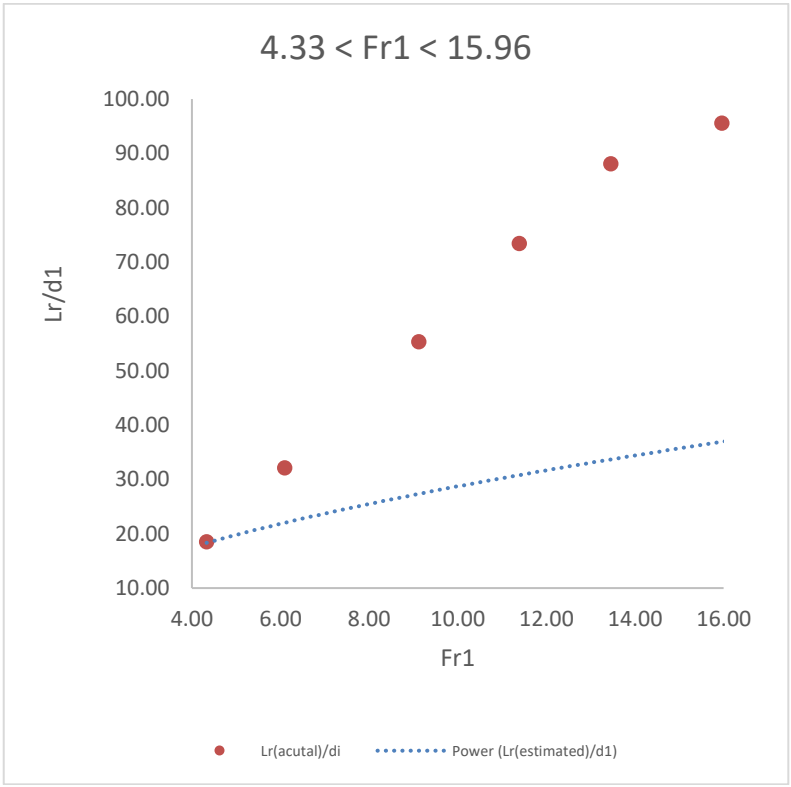

Fig. 3c. Froude number, Fr_1, of between 4.33 and 15.96 plotted as a function of the dimensionless hydraulic roller length, Lr(estimated)/d_1 and Lr(measured)/d_1, of between 96 and 36. The Pearson Correlation Coefficient is 1.00

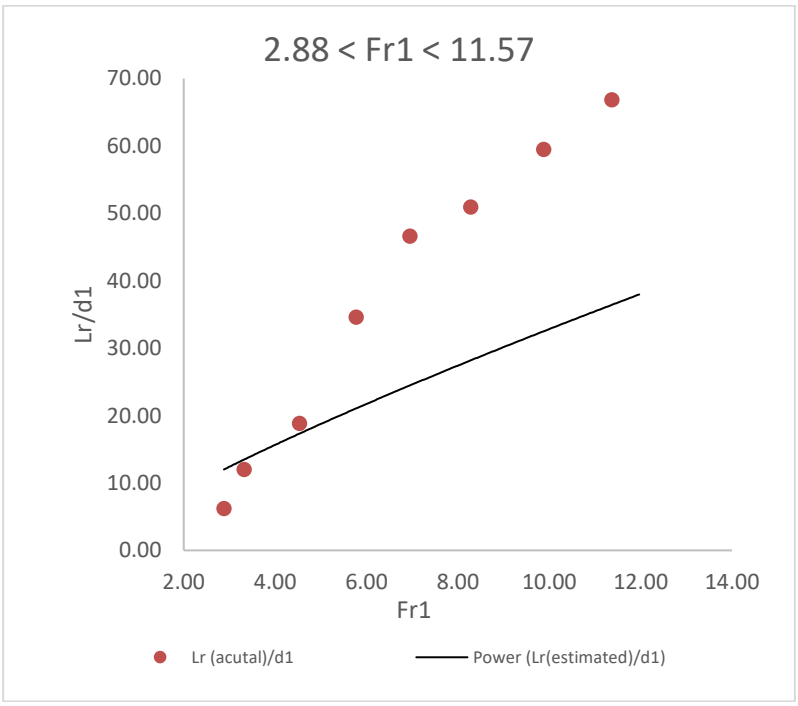

Fig. 3d. Froude number, Fr_1, of between 2.88 and 11.37 plotted as a function of the dimensionless hydraulic roller length, Lr(estimated)/d_1 and Lr(measured)/d_1, of between 67 and 36. The Pearson Correlation Coefficient is 0.98

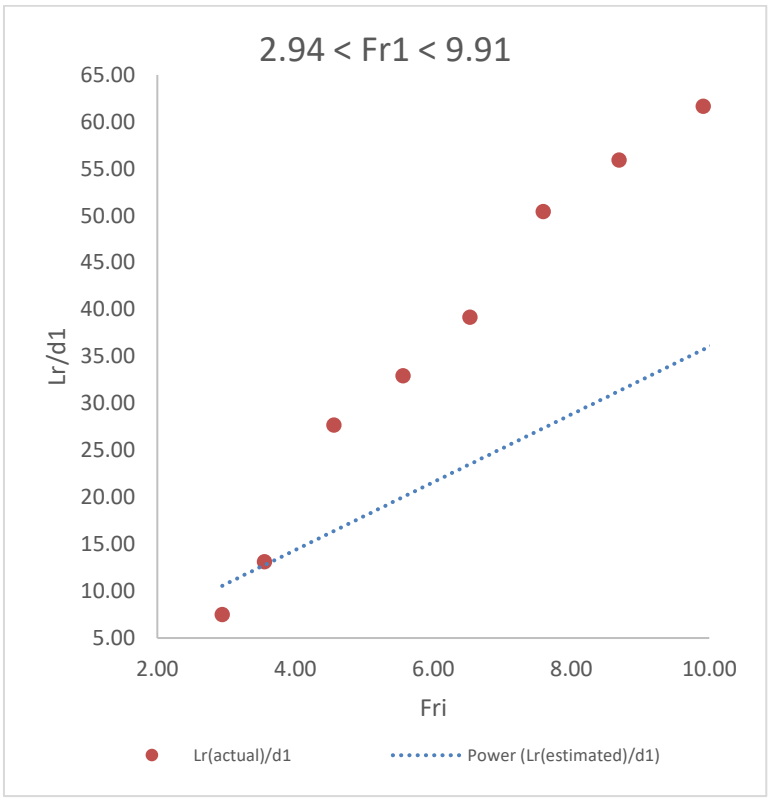

Fig. 3e. Froude number, Fr_1, of between 2.94 and 9.91 plotted as a function of the dimensionless hydraulic roller length, Lr(estimated)/d_1 and Lr(measured)/d_1, of between 62 and 34. The Pearson Correlation Coefficient is 1.00

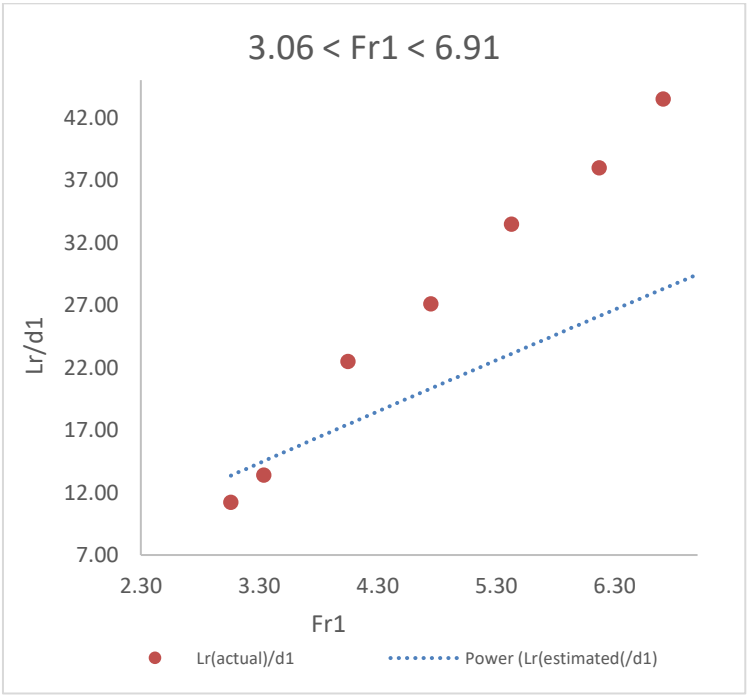

Fig. 3f. Froude number, Fr_1, of between 2.94 and 9.91 plotted as a function of the dimensionless hydraulic roller length, Lr(estimated)/d_1 and Lr(measured)/d_1, of between 62 and 34. The Pearson Correlation Coefficient is 1.00

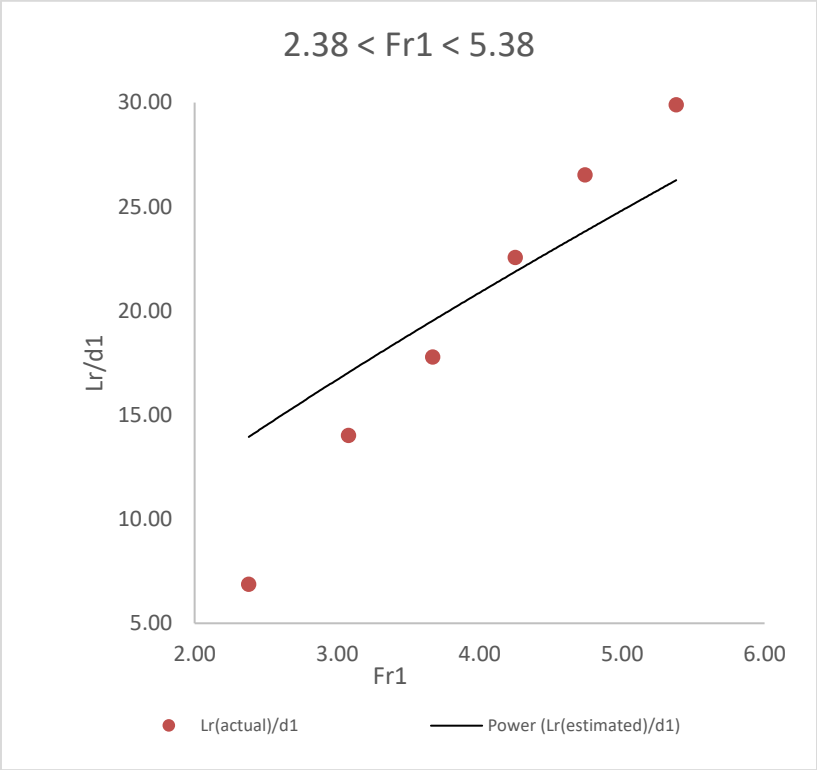

Fig. 3g. Froude number, Fr_1, of between 2.38 and 5.38 plotted as a function of the dimensionless hydraulic roller length, Lr(estimated)/d_1 and Lr(measured)/d_1, of between 30 and 36. The Pearson Correlation Coefficient is 0.93

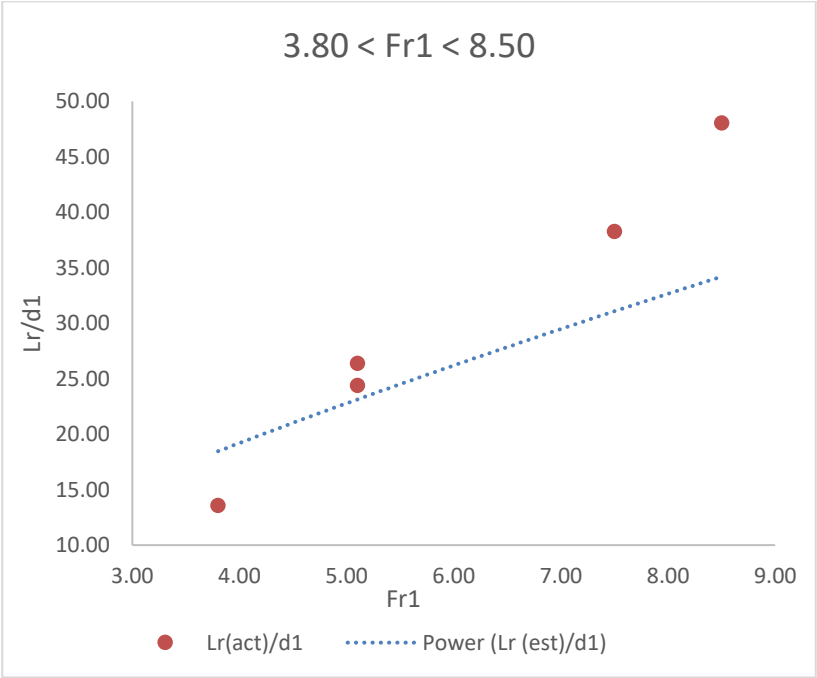

Fig. 3h. Froude number, Fr_1, of between 3.80 and 8.50 plotted as a function of the dimensionless hydraulic roller length, Lr(estimated)/d_1 and Lr(measured)/d_1, of between 10 and 50. The Pearson Correlation Coefficient is 0.98

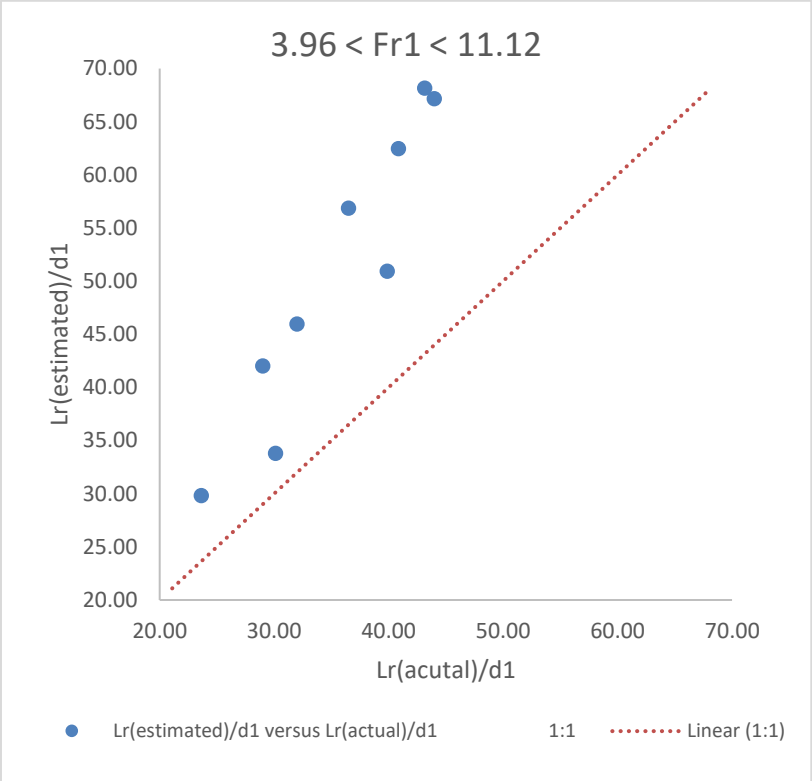

Fig. 4a. Dimensionless comparison between the calculated roller length of a hydraulic jump (Eq. 21) (vertical axis) and measured (horizontal axis) for Froude number, Fr_1, of between 2.96 and 11.12. The Pearson Correlation Coefficient is 1.00

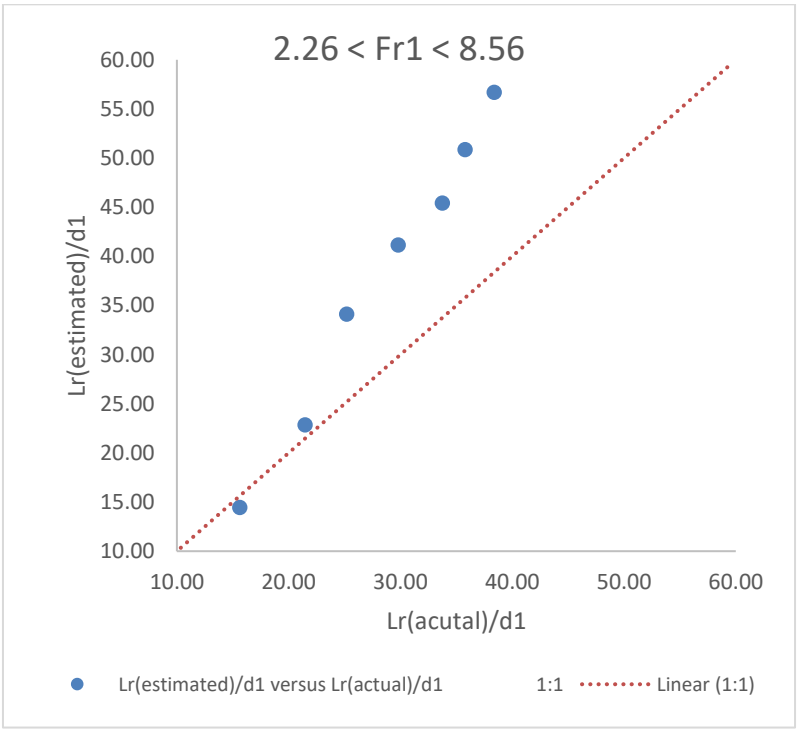

Fig. 4b. Lr(actual)/d_1 plotted as a function of Lr(estimated)/d_1 for Froude number, Fr_1, of between 2.96 and 11.12. The Pearson Correlation Coefficient is 1.00

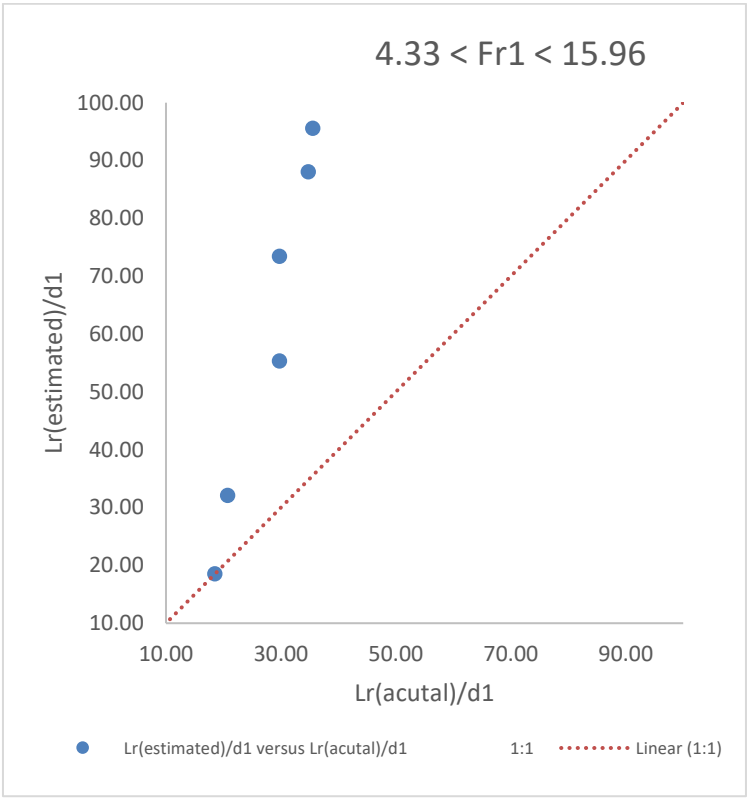

Fig. 4c. Lr(actual)/d_1 plotted as a function of Lr(estimated)/d_1 for the Froude number, Fr_1, of between 4.33 and 15.96. The Pearson Correlation Coefficient is 1.00

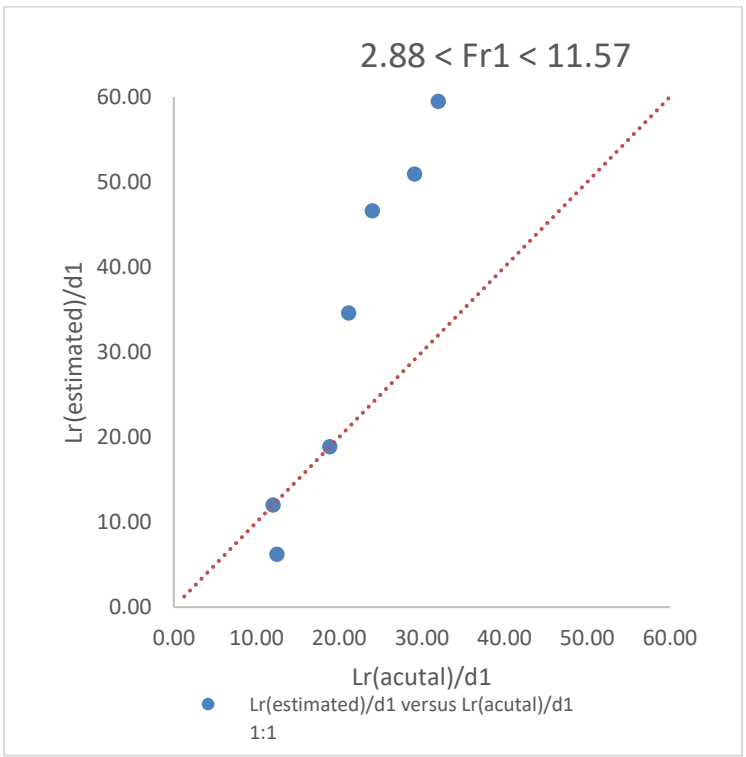

Fig. 4d. Lr(actual)/d_1 plotted as a function of Lr(estimated)/d_1 for Froude number, Fr_1, of between 2.88 and 11.37. The Pearson Correlation Coefficient is 0.98

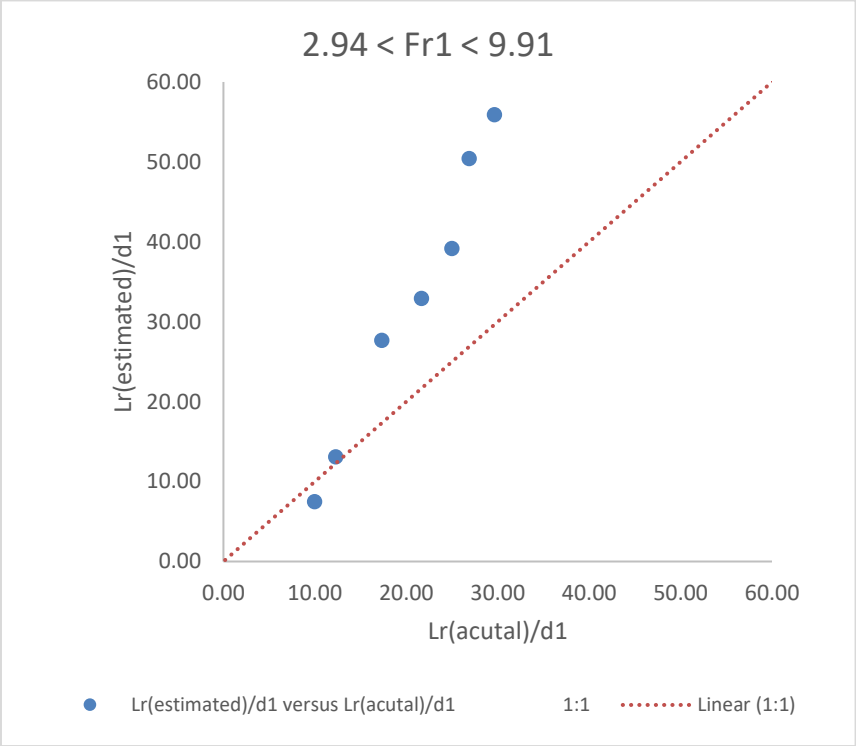

Fig. 4e. Lr(actual)/d_1 plotted as a function of Lr(estimated)/d_1 for Froude number, Fr_1, of between 2.94 and 9.91. The Pearson Correlation Coefficient is 1.00

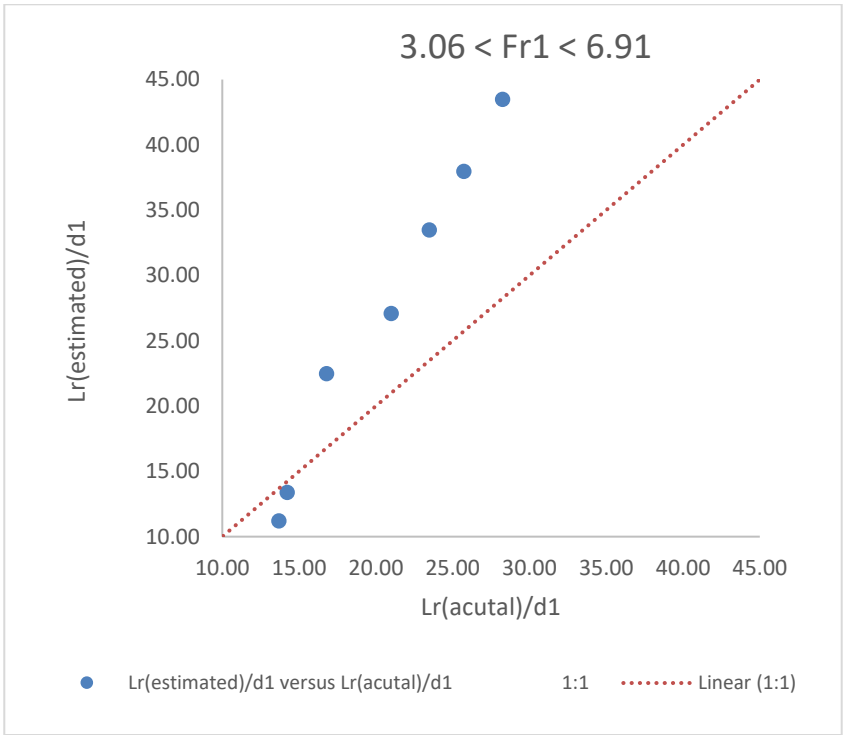

Fig. 4f. Lr(actual)/d_1 plotted as a function of Lr(estimated)/d_1 for Froude number, Fr_1, of between 3.06 and 6.71. The Pearson Correlation Coefficient is 0.99

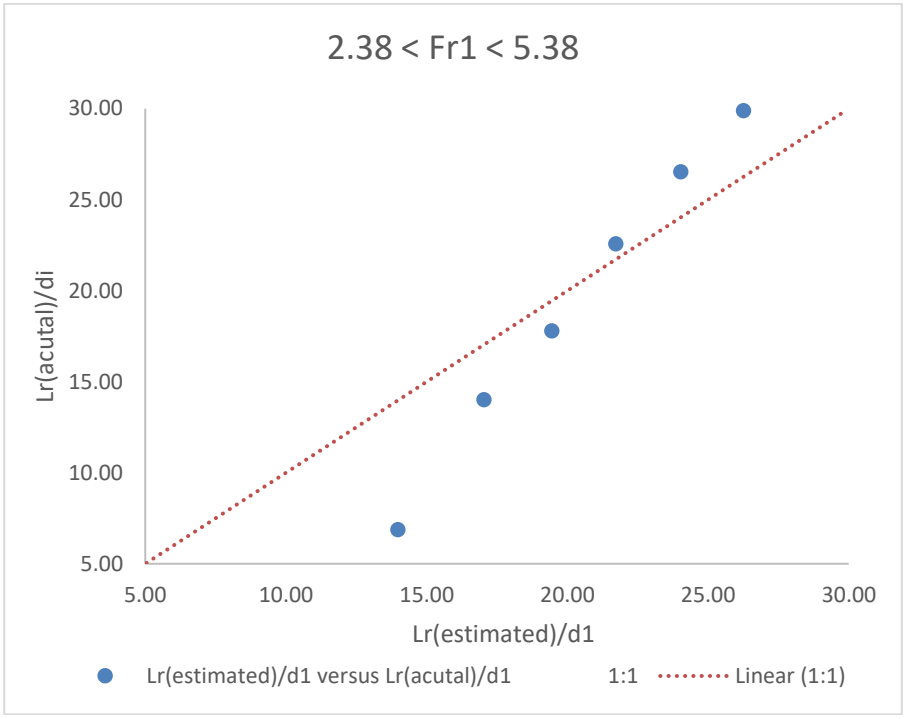

Fig. 4g. Lr(actual)/d_1 plotted as a function of Lr(estimated)/d_1 for Froude number, Fr_1, of between 2.38 and 5.38. The Pearson Correlation Coefficient is 0.99

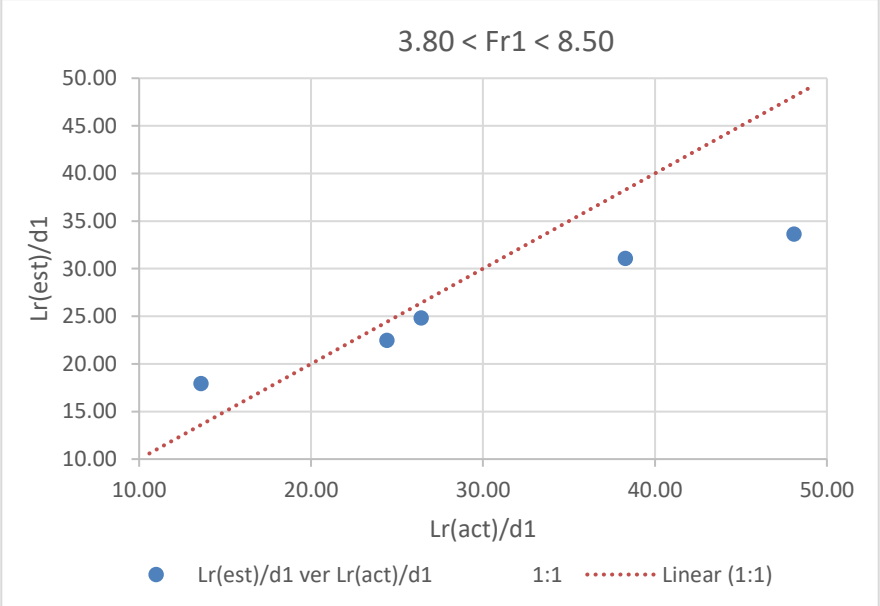

Fig. 4h. Lr(actual)/d_1 plotted as a function of Lr(estimated)/d_1 for Froude number, Fr_1, of between 3.80 and 8.50. The Pearson Correlation Coefficient is 0.95

7. CONCLUSION

The results show that a new model is developed to analytically calculate the roller length of a fully developed hydraulic jump in a horizontal open channel flow using a bouncing ball. The model is based on the laws of motion and the principles of impulse and momentum, to predict the roller length of a fully developed hydraulic jump in a horizontal open channel flow with the Froude number between 2.25 and 15.96. The model is then verified with the experimental roller length

obtained in a large-size facilities. The measured and the estimated dimensionless roller length of the hydraulic jump are virtually identical with each other and increase rapidly with the increasing Froude numbers, which is in line with reports recorded in the literature. The developed model (Eq 21) predict values of the roller length of hydraulic jumps that compare well the measured roller length with the Pearson correlation coefficients of between 0.93 and 1.00.

ACKNOWLEDGEMENT

We acknowledge the fruitful discussions with Prof Hubert Chanson of the Department of Civil Engineering, The University of Queenland, Brisbane QLD 4072 and Prof Cross Rodney of the Department of Physics, The University of Sydney, Sydney, NSW 2006, Australia

DISCLAIMER (ARTIFICIAL INTELLIGENCE)

Author(s) hereby declare that NO generative AI technologies such as Large Language Models (ChatGPT, COPILOT, etc) and text-to-image generators have been used during writing or editing of this manuscript.

COMPETING INTERESTS

Author has declared that no competing interests exist.

REFERENCES

Bakhmeteff, B. A., & Matzke, A. E. (1936). The hydraulic jump in terms of dynamic similarity. *Proceedings of the American Society of Civil Engineers, 61*(2), 145-162.

Bélanger, J. B. (1841). *Notes sur l'hydraulique* [Notes on hydraulic engineering]. Ecole Royale des Ponts et Chaussées, Paris, France, session 1841–1842.

Boor, B. (1960). Contribution au calcul de la longueur du ressaut hydraulique (Contribution to the Computation of the Length of Hydraulic Jump). *Vodohospodarsky Casopis Sav, 8*(4), 337-344.

Bradley, J. N., & Peterka, A. J. (1957). The hydraulic design of stilling basins: Hydraulic jumps on a horizontal apron (Basin I). *Journal of the Hydraulics Division, 83*(5), 1-24.

Busch, F. (1981). The length of the free plane hydraulic jump on a horizontal floor in regard to F. *XIX IAHR-Congress*, New Delhi, India, Subject D(b), Paper Nr. 15, 299-306.

Carollo, F. G., Ferro, V., & Pampalone, V. (2012). New expression of the hydraulic jump roller length. *Journal of Hydraulic Engineering, 138*(11), 995-999.

Chachereau, Y., & Chanson, H. (2010). Free-surface turbulent fluctuations and air-water flow measurements in hydraulic jumps with small inflow Froude numbers. *Hydraulic Model Report No. CH78/10*, School of Civil Engineering, The University of Queensland, Brisbane, Australia.

Chachereau, Y., & Chanson, H. (2011). Free-surface fluctuations and turbulence in hydraulic jumps. *Experimental Thermal and Fluid Science, 35*(6), 896-909.

Chanson, H. (2009). Current knowledge in hydraulic jumps and related phenomena: A survey of experimental results. *European Journal of Mechanics-B/Fluids, 28*(2), 191-210.

Chanson, H. (2010). Convective transport of air bubbles in strong hydraulic jumps. *International Journal of Multiphase Flow, 36*, 798-814.

Chanson, H., & Carvalho, (2015). Hydraulic jumps and stilling basins. In H. Chanson (Ed.), *Energy dissipation in hydraulic structures* (pp. 65–104). CRC Press. The Netherlands. https://doi.org/10.1201/b18441

Ciltrin, D. (1939). II risalto di Bidone [The hydraulic jump]. *L'Energia Elettrica, 16*, 441-465; 517-527.

Cross, R., & Crawford, L. (2019). Collision of a ball with the edge of a step. *European Journal of Physics*.

Cross, R., & Nathan, A. (2007). Experimental study of the gear effect in ball collisions. *American Journal of Physics, 75*.

Einwechter, J. (1932). Berechnung der Deckwalzenbreite des freien Wechselsprunges [Computation of roller length of free hydraulic jump]. *Wasserkraft und Wasserwirtschaft, 27*, 245-249.

Einwechter, J. (1935). Wassersprung und Deckwalzenlange [Hydraulic jump and length of roller]. *Wasserkraft und Wasserwirtschaft, 30*, 85-88.

Felder, S., & Chanson, H. (2017). Scale effects in microscopic air-water flow properties in high-velocity free-surface flows. *Experimental Thermal and Fluid Science, 83*, 19-36.

Felder, S., & Chanson, H. (2018). Air-water flow patterns of hydraulic jumps on uniform bed

macro-roughness. *Journal of Hydraulic Engineering, 144*(3), 04017068.

Felder, S., Montano, L., Cui, H., Peirson, W., & Kramer, M. (2021). Effect of inflow conditions on the free-surface properties of hydraulic jumps. *Journal of Hydraulic Research*. https://doi.org/10.1080/00221686.2020.1866692

Fiorotto, V., & Rinaldo, A. (1992). Turbulent pressure fluctuations under hydraulic jumps. *Journal of Hydraulic Research, 30*(4), 499-520.

Giles, R. V., Evett, J. B., & Liu, C. (1994). *Schaum's outline of fluid mechanics and hydraulics* (3rd ed.). McGraw-Hill Press.

Glen, S. (2020). Alpha level (significance level): What is it? *StatisticsHowTo.com*. https://www.statisticshowto.com/probability-and-statistics/statistics-definitions/what-is-an-alpha-level/

Hager, R., Bremen, N., & Kawagoshi, N. (1990). Classical hydraulic jump: Length of roller. *Journal of Hydraulic Research, 28*(5), 591-608. https://doi.org/10.1080/00221689009499048

Hager, W. H. (1992). *Energy dissipators and hydraulic jump*. Kluwer Academic Publishers. Netherlands.

Hager, W. H., & Bremen, R. (1989). Classical hydraulic jump: Sequent depths. *Journal of Hydraulic Research, 27*(5), 565-585.

Hoyt, J. W., & Sellin, R. H. J. (1989). Hydraulic jump as "mixing layer". *Journal of Hydraulic Engineering, 115*(12), 1607-1614.

Kobus, H. (Ed.). (1980). *Hydraulic modelling* (Bulletin 7). German Association for Water Resources and Land Improvement, Parey, Hamburg.

Kramer, M., & Valero, D. (2020). Turbulence and self-similarity in highly aerated shear flows: The stable hydraulic jump. *International Journal of Multiphase Flow, 129*.

Kramer, M., Chanson, H., & Felder, S. (2020). Can we improve the non-intrusive characterization of high-velocity air-water flow? Application of LIDAR technology to stepped spillways. *Journal of Hydraulic Research, 58*(2), 350-362.

Kucukali, S., & Chanson, H. (2008). Turbulence measurements in the bubbly flow region of hydraulic jumps. *Experimental Thermal and Fluid Science, 33*(1), 41-53.

Leng, X., & Chanson, H. (2015). Turbulent advances of a breaking bore: Preliminary physical experiments. *Experimental Thermal and Fluid Science, 62*, 70-77.

Leutheusser, H. J., & Alemu, S. (1979). Flow separation under hydraulic jump. *Journal of Hydraulic Research, 17*(3), 193-206.

Li, R., Splinter, K., & Felder, S. (2020). Time-varying free-surface properties of hydraulic jumps: A comparative analysis of experimental methods. *arXiv:2007.05128*.

Li, R., Splinter, K., & Felder, S. (2021). Aligning free surface properties in time-varying hydraulic jumps. *Experimental Thermal and Fluid Science, 126*. Aligning free surface properties in time-varying hydraulic jumps. https://doi.org/10.1016/j.expthermflusci.2021.110392

Montano, L., & Felder, S. (2018, December). Effect of inflow conditions on the air-water flow properties in hydraulic jumps. *Proceedings of the 21st Australasian Fluid Mechanics Conference*, Adelaide, Australia.

Montano, L., & Felder, S. (2020). LIDAR observations of free-surface time and length scales in hydraulic jumps. *Journal of Hydraulic Engineering, 146*(4), 04020007.

Montano, L., Li, R., & Felder, S. (2018). Continuous measurements of time-varying free-surface profiles in aerated hydraulic jumps with a LIDAR. *Experimental Thermal and Fluid Science, 93*, 379-397.

Mossa, M. (1999). On the oscillating characteristics of hydraulic jumps. *Journal of Hydraulic Research, 37*(4), 541-558.

Mozer, A., & Sevam, H. (2024). Investigating the influence of vegetation height on the air concentration of supercritical aerated flows. *Water, 16*(21). https://doi.org/10.3390/w16213136

Murzyn, F., & Chanson, H. (2009). Free-surface fluctuations in hydraulic jumps: Experimental observations. *Experimental Thermal and Fluid Science, 33*(7), 1055-1064.

Ohtsu, I., & Yasuda, Y. (1994). Characteristics of supercritical flow below sluice gate. *Journal of Hydraulic Engineering, 120*(3), 332-346.

Ozueigbo, O. (2021). *Analysis of flow and the energy dissipation down a stepped spillway* (Ph.D. thesis). University of Nigeria, Nsukka.

Ozueigbo, O., & Agunwamba, J. (2023). New equations for rate of energy dissipation of

a stepped spillway with slope less than critical and specific step height. *Journal of Engineering Research and Technology, 10*(2), 49-57. https://doi.org/10.33976/JERT.10.2/2023/2

Ozueigbo, O., & Agunwamba, J. (2023). New equations for rate of energy dissipation of a stepped spillway with slope less than critical and specific step height. *Journal of Engineering Research and Technology, 10*(2), 49-57. https://journals.iugaza.edu.ps/index.php/JERT/issue/view/352.Slope less than Critical and Specific Step Height. https://doi.org/10.33976/JERT.10.2/2023/2

Peterka, A. J. (1978). *Hydraulic design of stilling basins and energy dissipators*. Denver, CO, USA: 1978.

Rajaratnam, N. (1965). The hydraulic jump as a well jet. *Journal of the Hydraulics Division, 91*(5), 107-132.

Rajaratnam, N. (1967). Hydraulic jumps. In *Advances in hydroscience, 4*, 197-280.

Rouse, H., Siao, T. T., & Nagaratnam, S. (1959). Turbulence characteristics of the hydraulic jump. *Journal of the Hydraulics Division, 84*(1), 1-30.

Safranez, K. (1929). *Untersuchungen über den Wechselsprung* [Studies on the hydraulic jump]. Selbstverlag.

Sarma, K. V. N., & Newnham, D. A. (1973). Surface profiles of hydraulic jump for Froude numbers less than critical. *Journal of Hydraulic Research, 17*(3), 193-206.

Schroder, R. (1963). *Die turbulente Strömung im freien Wechselsprung* [The turbulent flow in the free hydraulic jump]. Teilung Nr. 59, Berlin.

Wang, H., & Chanson, H. (2015b). Experimental study of turbulent fluctuations in hydraulic jumps. *Journal of Hydraulic Engineering, 141*(7).

Wang, H., & Chanson, H. (2016). Self-similarity and scale effects in physical modelling of hydraulic jump roller dynamics, air entrainment and turbulent scales. *Environmental Fluid Mechanics, 16*, 1087-1100.

Zhang, G., Wang, H., & Chanson, H. (2013). Turbulence and aeration in hydraulic jumps: Free-surface fluctuation and integral turbulent scale measurements. *Environmental Fluid Mechanics, 13*(2), 189-204.

Peer-review history:
The peer review history for this paper can be accessed here:
https://www.sdiarticle5.com/review-history/127641